Precision Engineering 37 (2013) 129–134

Contents lists available at SciVerse ScienceDirect

Precision Engineering

journal homepage: www.elsevier.com/locate/precision

Mechanics of the burnishing process

Pascale Balland [a], Laurent Tabourot [a,*], Fabien Degre [a], Vincent Moreau [b]

[a] Université de Savoie, Laboratoire SYMME, BP 80439, 74944 Annecy-le-Vieux Cedex, France
[b] Centre Technique du Décolletage, BP 65, 74301 Cluses Cedex, France

ARTICLE INFO

Article history:
Received 12 March 2012
Received in revised form 12 July 2012
Accepted 16 July 2012
Available online 23 July 2012

Keywords:
Roller burnishing
Deep rolling
Finite element method
Contact mechanics

ABSTRACT

Burnishing is a low-cost surface treatment process. However, scientific studies on this process have so far failed to describe how the process leads to surface hardening and improvement in the geometric quality of the material. Indeed, in spite of its apparent simplicity the process is rather complicated to reproduce by numerical simulation. This paper proposes a finite element modelling of the ball burnishing process. Thanks to this model, the effect of the burnishing process on the material is analysed. A ridge phenomenon that affects the mechanics of the process is demonstrated, allowing for improved modelling of the burnishing process.

1. Introduction

Burnishing is an industrial process used to confer extra mechanical and geometrical properties to machined metallic pieces on a lathe. It is often used as a final machining operation in order to avoid supplementary and costly operations on other machines such as grinders.

Burnishing proceeds by crushing the surface irregularities generated by machining with a rotating cylindrical or spherical roller. This latter element is free to rotate about its axis. It is pushed against the rotating machined part and translated along a generatrix. The concentrated pressure generated by the localised contact with the roller is accommodated by plastic deformations of the surface irregularities which tend to make the surface smoother. In addition, the localisation of these plastic deformations in a thin superficial layer produces compressive residual stresses that increase the resistance of the piece to fatigue [1]. Furthermore, the surface hardness is increased by the resulting hardening of the material [2]. Nevertheless, a desired hardness or roughness is difficult to obtain because there is no direct link between the operating parameters and the induced effects on these mechanical properties. Scientists propose various methods to better predict the effects of the process parameters. Thus, the effects of various parameters (such as the initial surface roughness and hardness of the workpiece, the burnishing tool geometry, and the lubricant) on hardness were systematically studied on two non-ferrous workpiece materials by Loh et al. [3] and Hassan and Maqableh [4].

Prediction of ball burnishing geometrical and mechanical effects falls into the problem category of mechanics of deformable media with boundary limits.

Hassan and Al-Bsharat [5], El-Axir [6], Luca et al. [7], El-Tayeb et al. [8] and López de Lacalle et al. [9] provide models determined by empirical procedures. The validity of each of these experimental models is therefore limited to a particular configuration. Hence, it is difficult to apply them to other cases.

To obtain a more general model of the process, it is necessary to obtain a clear representation of the principal deformation mechanisms. The fundamental elementary mechanisms that are involved during burnishing are mainly those involved in spherical contact. Based on strong simplifying assumptions, Luo et al. [10] proposed an analytical model of the burnishing operation.

However, as the process induces highly nonlinear local strains, finite element modelling is unavoidable to obtain a more generalized model. In spite of the apparent simplicity of the process, a finite element model of ball burnishing involves very refined meshes and complex boundary limits. Therefore, all the studies in this field are concerned with methods to reduce the size of the problem and use simplified boundary conditions.

Röttger [11] used a numerical modelling approach to simulate the effect of the ball burnishing process. The simulation is limited to the radial plane of the turned part defined by the axis of the part and the generatrix, followed by the roller. Hence, three assumptions are used in order to reduce the problem to a 2D model: (1) the plane strain hypothesis is adopted, (2) strains are localized in the thin superficial layer and (3) the continuous sweeping of the roller over

* Corresponding author. Tel.: +33 450 096 563; fax: +33 450 096 543.
E-mail addresses: pascale.balland@univ-savoie.fr (P. Balland), laurent.tabourot@univ-savoie.fr (L. Tabourot), v.moreau@ctdec.com (V. Moreau).

0141-6359/$ – see front matter © 2012 Elsevier Inc. All rights reserved.
http://dx.doi.org/10.1016/j.precisioneng.2012.07.008

the piece is equivalent to incrementally shifted indentations which correspond to the displacement of the roller after each revolution of the piece. Röttger found that this 2D model, monitored by the force imposed on the roller, underestimates the penetration depth of the rolling element due to the overestimation of the contact surface area with the plane strain assumption. Indeed the portion of the roller in contact with the piece can be approximated by a portion of a sphere whereas the hypothesis assumes contact with an infinite cylinder.

Yen et al. [12] developed a new model based on Röttger's work. The improvement consisted in controlling the position of the rolling element while still invoking the plane strain assumption in the case of a refined 2D model. The penetration depth of the rolling element is previously determined by a fully three-dimensional (3D) simulation of the rolling tool acting on a parallelepiped representing a portion of the surface layer of the piece. The residual stresses are compared with the experimental values and the results, unexpectedly, show a greater degree of correlation with the 2D model than with the 3D model.

The dispersion of the results and the difficulty in explaining some of them should lead to a reconsideration of the initial assumptions. These assumptions were applied in order to reach a reasonable ratio between simulation time and quality of the results. Thus, less reductive assumptions should be applied in order to improve the quality of the result even if more computer time is required. The first assumption (1) cannot fully be applied in the case of ball burnishing or burnishing by a cylinder of which the axis is inclined relative to the axis of the piece. The assumption (3) made by Röttger must also be questioned. In this paper, the response of the material to burnishing is studied with less constrained assumptions. The full tri-dimensional state of the problem is assumed even if the price to pay is highly time consuming simulations. Two 3D numerical models are therefore proposed in this paper. The first model deals with burnishing a perfectly smooth cylinder. The second model analyses the effect of surface irregularities on the mechanics of burnishing. These irregularities are produced by machining. To ensure optimal comparison, both models are built following the same scheme.

2. 3D modelling of the burnishing process

The first model deals with the burnishing of a smooth cylinder by a ball. Only a portion of the surface layer of the piece is taken into account in the model and is sufficient to obtain representative results (Fig. 1). The diameter of the burnished piece is assumed to be sufficiently large with respect to the diameter of the roller so that the considered portion of layer can be considered flat in the numerical model. For the other model dealing with the interaction of the roller with rough surfaces the same considerations are applied. The surface is generated by extrusion of a periodic triangular profile whose characteristics correspond to those generated by machining on a real piece. The dimensions of the considered portions of layer are set as small as possible so that the stress state remains identical when they are increased. The ball is modelled as an analytical surface.

The representative portion of the burnished piece is discretised into 300,085 Lagrangian tetrahedral elements with four nodes (linear function). A meshing program based on the computation of an error estimator is used to optimise the element density. Until this error estimator exceeds a user-set upper bound, both the size and the distribution of the elements are refined. The finite element code ABAQUS used in this study computes an error estimator following [13]. A detailed description of the technique is to be found in [14]. As computation of this numerical model is already highly time-consuming, the upper bound of the error estimator is set as high as possible in order to obtain a solution that, on the one hand, is not dependant on the mesh and, on the other hand, induces the smallest computation time. The remaining part of the piece, which has no impact on the results, is modelled by 4891 semi-infinite linear elements. In the software, the semi-infinite elements are only available in the hexahedral form therefore a transition zone between tetrahedral and hexahedral elements is built on the periphery of the useful refined volume. The discretisation of the piece is shown in Fig. 2.

The x, y and z directions correspond respectively to the tangential direction of displacement, the direction normal to the surface and the direction tangentially perpendicular to the direction of displacement.

The model chosen to represent the mechanical behaviour of the material is an elastic–plastic one. The parameters of this model and the techniques used for their identification are given in Table 1. The hardening curve has been experimentally obtained on classical industrial steel (11SMn30) and is given in Fig. 3. The rolling element is considered to be perfectly rigid.

The movement of the ball is composed of four regularly shifted identical trajectories, each of them consisting of four similar steps. The first step is a penetration (or indentation) step into the material, during which the ball undergoes a normal displacement into the surface (y direction) to reach a given depth. The second step is characterised by an x displacement of the roller at a constant depth in the y direction. Then, two supplementary steps are needed to shift and position the ball for the next cycle. The corresponding displacements of the ball and its degrees of freedom are given in

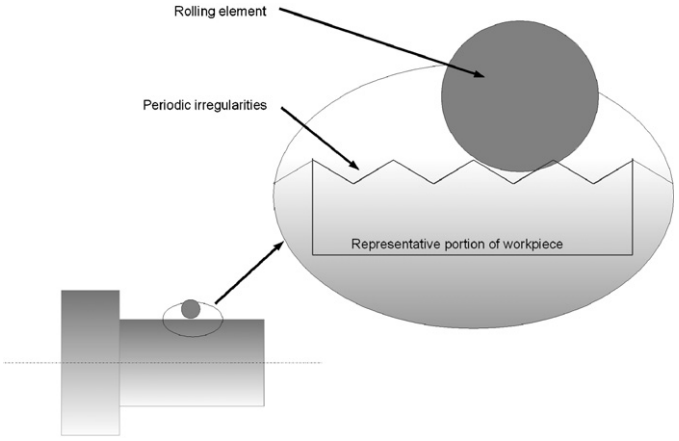

Fig. 1. Localization of the representative portion of the piece used in the finite element simulation of ball burnishing.

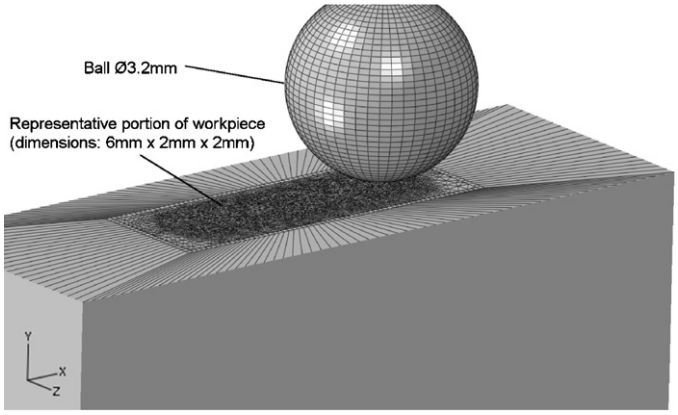

Fig. 2. Geometric models and meshes of the portion of layer and the roller for the case of burnishing of smooth cylinder by a ball.

Table 1
Summary of the constitutive models for the material behavior, the method of characterization and the corresponding identified parameters.

Phenomenon	Model	Method of determination	Identified values
Elasticity	Classic Hooke's law	Time of flight measurement of an ultrasonic wave	Isotropic E = 199 GPa nu = 0.30
Plasticity	Von Mises' plasticity criteria	Compression test ("Rastegaev" geometry) see Fig. 3	Initial yield stress Re = 151 MPa
Plasticity	Hardening law		Isotropic
Plasticity	Flow law		Associated

Table 2
Displacements and freedom degrees of the ball for the 3D simulation of burnishing with a ball for a given trajectory.

	U_x (mm)	U_y (mm)	U_z (mm)	U_{Rx}	U_{Ry}	U_{Rz}	Time (s)
Step 1: normal penetration	0	−0.01	0	0	0	0	0–1
Step 2: rolling (burnishing phase)	−4	0	0	0 if μ = 0, otherwise free	0	0	1–2
Step 3: ascent	0	0.01	0	0	0	0	2–3
Step 4: backwards and shift	−4	0	0.2	0	0	0	3–4

Table 2. U_x, U_y and U_z represent the translations in the x, y and z directions, respectively; U_{Rx}, U_{Ry} and U_{Rz} represent the rotations around the x, y and z directions, respectively.

μ is the coefficient of friction between the ball and the burnished surface. The contact is managed by a hard master-slave contact algorithm. The problem is solved by supposing a quasi-static equilibrium and therefore by adopting an implicit Newtonian integration method (ABAQUS/Standard). Large rotations are taken into account using the NLGEOM option.

Considered together, the results of successive initial indentations can be used as reference. They are assumed to reproduce elementary effects of burnishing as was proposed in Refs. [11,12]. It is of interest therefore to compare the effects of these indentations to the effects of full 3D burnishing.

3. Results and discussion

3.1. Ball burnishing of a smooth cylinder

Initially, the friction coefficient μ is set to zero. Thus, only normal forces are transmitted between the ball and burnished part.

The evolution of the resulting force components during the first trajectory of the ball is given in Fig. 4. The time for each step describing the trajectory of the ball is arbitrarily one second. The interval [0 s,1 s] corresponds to the penetration phase (step 1), and the interval [1 s, 2 s] corresponds to the burnishing phase (step 2).

In the early stages of rolling, during the interval [1 s, 1.1 s], the absolute value of the normal force F_y tends to decrease. This is due to the release of the rolling element from the footprint generated by the indentation/penetration phase. After this phase, the amplitude of the force increases gradually until it stabilises at a value that is close to the one obtained at the end of the indentation phase.

To complete the analysis of the forces transmitted by the ball on the piece, the pressure distribution is studied on the contact elements between the ball and the piece thanks to the output of ABAQUS. Figs. 5 and 6 show the contact pressure distributions in the contact area for indentation phase and burnishing phase respectively. These graphs show the amplitudes of the pressure for each

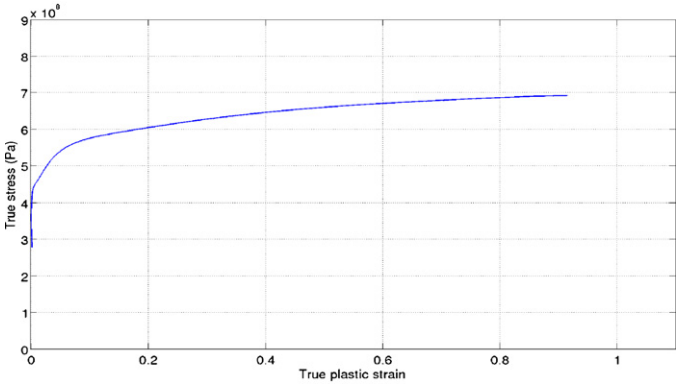

Fig. 3. Experimental hardening curve of 11SMn30 issued from a cylinder compression test.

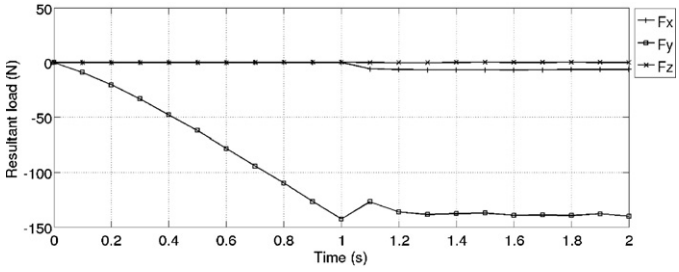

Fig. 4. Evolutions of resulting force components on the ball during the penetration phase [0 s, 1 s] and during the burnishing phase [1 s, 2 s].

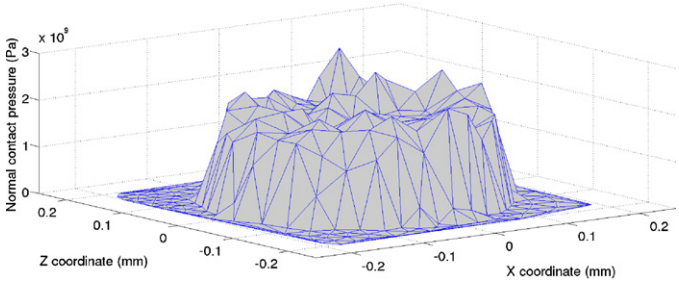

Fig. 5. Pressure distribution at the end of the indentation phase.

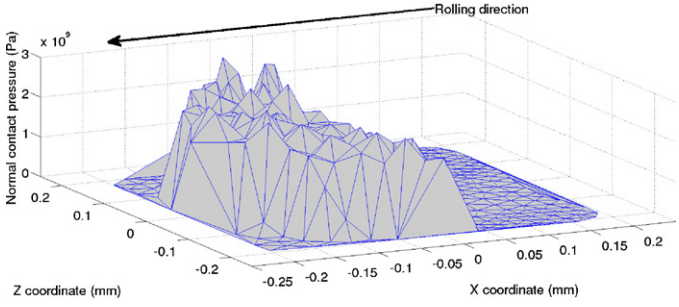

Fig. 6. Pressure distribution in the contact zone during stabilized burnishing phase.

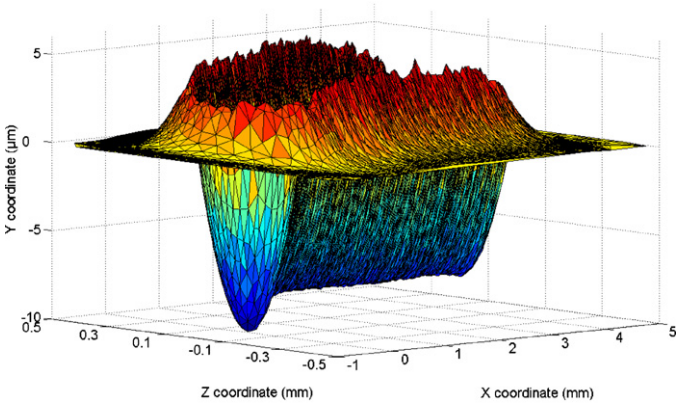

Fig. 7. Topology of the surface under the stress of rolling contact.

element of the surface in contact with the ball. The coordinates x and z are measured from the centre of the ball. The pressures generated by indentation phase are axisymmetric around the indentation axis (y axis) (cf. Fig. 5). When the burnishing phase is stabilized, the small discrepancies are observed in Fig. 6 only due to the errors associated with discretisation. The contact tends to be localized at the front of the ball. Only a small contact area exists behind the ball: it is due to elastic springback of the material. The pressure amplitudes are nearly the same as those during indentation phase.

Fig. 7 shows the topology of the surface during stabilized burnishing. The x and z coordinates are centred on the centre of the ball. A ridge is clearly visible in the region upstream of the contact zone (negative x coordinates). During the ball displacement, the ridge is rejected in the z direction to form a protrusion on each side of the created groove. In the case presented here, the heights of the protrusions are greater than the height of the front ridge. In addition, the heights of the protrusions reach almost half of the depth of the groove.

This phenomenon is of paramount importance for understanding the mechanics of the burnishing process because the creation of lateral protrusions at each passage of the ball has clearly an impact on the final surface geometry of the burnished surface. Indeed, the protrusions arising on the side of the groove will have a complex interaction with the ball during the next trajectory.

Fig. 8 shows a section of the deformed surface in the yz plane located half-way along the first trajectory of the ball. As indicated, for comparison purposes, the profile of the surface at the end of the indentation phase is also plotted in this figure.

During the second trajectory, the generation of the protrusions is perturbed by the already existing one. Furthermore the second passage of the ball tends to raise the bottom of the groove created by the first passage. This phenomenon does not exist in the case of the indentation phases. Therefore, an important and paradoxical conclusion regarding the operation of burnishing can be inferred: in the simulated conditions, the passage of the rolling element tends to regenerate roughness on the surface that was smoothed in the previous round.

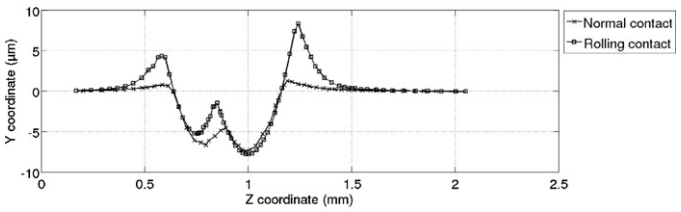

Fig. 8. Comparison of the surface profiles generated by indentation phase (normal contact) and burnishing phase (rolling contact) after the second trajectory.

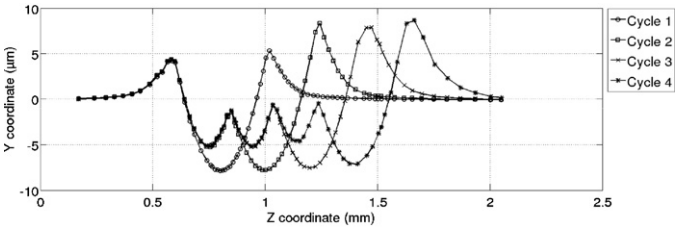

Fig. 9. The evolution of surface profiles in a plane parallel to (yOz) during each cycle of rolling contact in the case of a smooth surface.

Fig. 9 shows the profile of the surface generated by rolling contact at the end of each cycle and thus well illustrates this phenomenon. Thus, the stress from rolling contact presents an evolutionary characteristic at the initiation of rolling, and it does so during the first successive passes. A second remarkable conclusion on the behaviour of the burnishing process is that the burnishing process requires several rounds to reach steady state behaviour.

So far, the study of rolling contact was conducted under the assumption of zero friction. To assess the impact of this parameter on the mechanics of the operation, a simulation was conducted assuming a friction coefficient $\mu = 0.2$.

The geometry of the surface obtained when friction occurs between ball and piece is compared to the geometry of the surface shown in Fig. 7. For both cases, a half surface is analysed and is considered symmetric. The two half surfaces are presented side by side in Fig. 10. The data in the left side of the graph (positive z coordinates) correspond to the case $\mu = 0.2$ and the data in the right side (negative z coordinates) correspond to the case $\mu = 0$.

The friction coefficient seems to have a significant impact on the formation and flow of the ridge, especially on the surface geometry. The differences are measured primarily in the height of the ridge. In front of the ball, the height of the ridge is 2.8 µm for the frictionless case and 2 µm for the case with friction. This difference affects the heights of the lateral projections with a height of 5.3 µm for the case $\mu = 0$ and a height of 4.4 µm for the case $\mu = 0.2$. Friction appears to have a reducing effect on the formation and flow of the ridge. When increasing the friction at the interface of the rolling element and the piece, the generation of irregularities on the distorted surface piece should be reduced, thus improving the geometry of the burnished surface.

3.2. Consequences for an irregular surface

Real surfaces are rarely perfectly smooth. The processes for obtaining these surfaces always generate irregularities of varying amplitudes. Thus, the impact of the phenomena of formation and

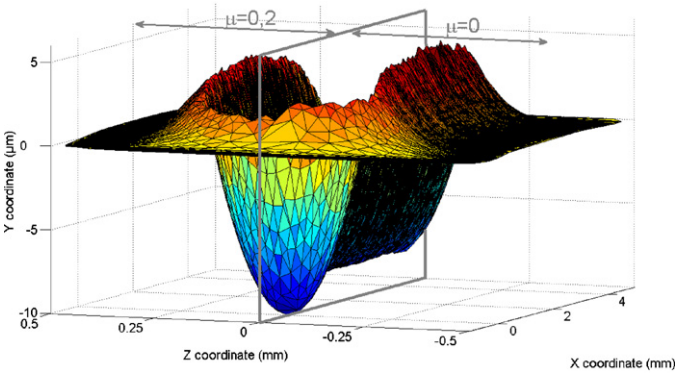

Fig. 10. A comparison of the topologies of smooth surfaces for rolling contact stress with a friction coefficient $\mu = 0$ (right: values for $z < 0$) and a friction coefficient $\mu = 0$ 2 (left: values for $z > 0$).

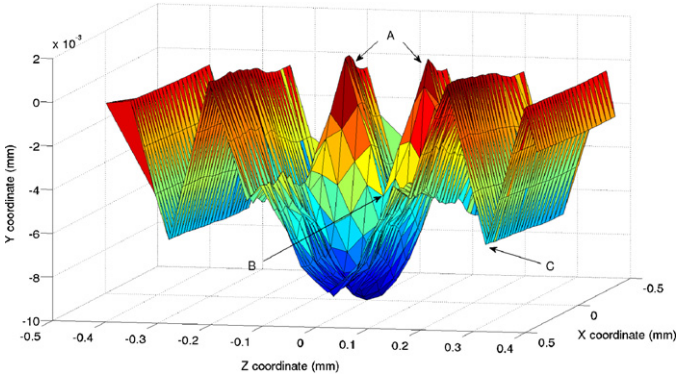

Fig. 11. Topology of a surface with periodic irregularities stressed by rolling contact (simulation); view 1.

flow of the ridge on the geometry of these irregularities should be investigated. Additional simulations were performed that considered periodic irregularities on the surface of the piece similar to those generated by a turning operation (in frequency and geometry). The roughness, inspired by experimental measurements, is constructed by the extrusion of a triangular periodic profile of 6.5 μm height and a period of 0.15 mm.

Figs. 11 and 12 show two views of the topology of a single surface generated by burnishing by a ball with friction. The x and y coordinates are centred on the centre of the ball. The ball is initially positioned directly above the bottom of a groove. The data are collected in the first trajectory.

Unlike the case of contact with smooth surfaces, the front ridge is not clearly identifiable. Indeed, only slight increases in the heights of the peaks are shown in Fig. 11 (zone A). However, the bottom of the groove, which is downstream from the contact, seems to have rebounded significantly (Fig. 11, zone B) from the bottom of the undistorted grooves (Fig. 11, zone C). Before the ball comes into contact with an irregularity, the geometry of the irregularity has already evolved. Therefore, the compressive action of the ball is applied to a surface whose shape and amplitude of irregularities are different from those of the initial surface.

A similar observation is made on the flow of the ridge. Fig. 12 (zones D) shows that the elevations of the adjacent peaks are only slightly changed by the passage of the ridge. However, the bottoms of the adjacent grooves have substantially rebounded (zones E).

In the next cycle (representing the second pass of the piece), the ball comes into contact with an irregularity whose geometry has been modified twice. The first modification occurred during the previous pass by the flow of the ridge, and the second modification occurred during the current pass through the action of the ridge

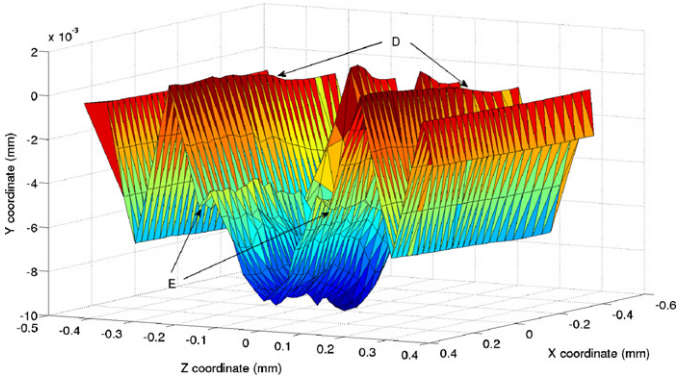

Fig. 12. The topology of a surface with periodic irregularities stressed by rolling contact (simulation); view 2.

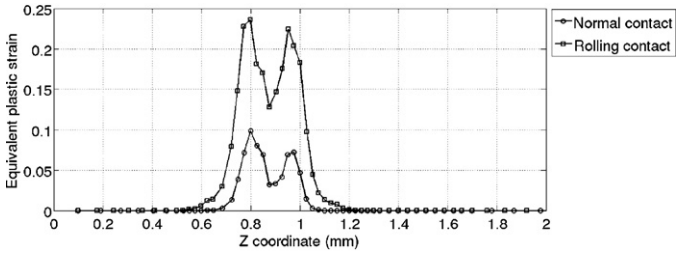

Fig. 13. Comparison of equivalent plastic strain in two planes parallel to (yOz) corresponding to indentation and burnishing phases.

front. Depending on the geometry of the surface and the size of the rolling element, the flow of the ridge likely interferes with any irregularities located at either small or large distances. The number of successive changes experienced by an irregularity before coming into contact with the tool can change.

To complete the analysis of the impact of the mechanism of ridge formation and flow, the equivalent plastic strain after burnishing is viewed with respect to the equivalent plastic strain after indentation. Fig. 13 shows the strain hardening (equivalent plastic strain) in a profile of the surface in two planes parallel to the (yOz) plane, one located at the centre of the ball caused by the indentation phase (first stage of rolling contact) and the other located in the middle of the path ahead of the ball in an area under steady-state loading. The data were collected during the first of the four cycles.

The overall evolution of the profiles is similar. In both cases, maximum strain-hardening is expected in the elements initially constituting the protrusion. Once again, a significant difference in the amplitudes between the two cases is noticed. The profiles have maximum values of equivalent plastic strain of 10% for indentation and 23.5% for burnished state.

4. Conclusion

In this work, the mechanics of the burnishing process using a ball have been studied in detail using 3D numerical models. The cost in computing time is important (about one week on an 8-CPU cluster node) but it is the price to pay to account for all the mechanisms involved in the burnishing process. A mechanism of formation and flow of the ridge has been demonstrated in accordance with experimental observations of [15]. For the case of smooth surfaces, this phenomenon plays an important role in the deformation of the surface. The consequences (geometrical and mechanical) of this phenomenon on an uneven surface were also presented. The mechanism of formation and flow of the ridge appears to have a central role in the treatment of a surface by burnishing. The numerical models of roller burnishing that are based on the assumption of equivalence between burnishing (rolling contact) and indentation phase (normal contact) are inadequate to provide an accurate estimation of the geometrical and mechanical characteristics of a roller-burnished surface. In our future work, we plan to use that model to identify the impact of multiple conditions on the ridge phenomenon.

Acknowledgements

Calculations of this study were performed in the laboratory LAPP at the CNRS – Université de Savoie calculation meso-centre MUST.

References

[1] Nalla R, Altenberger I, Noster U, Liu G, Scholtes B, Ritchie R. On the influence of mechanical surface treatments – deep rolling and laser shock peening – on the fatigue behavior of Ti–6Al–4V at ambient and elevated temperatures. Materials Science and Engineering A 2003;355:216–30.

[2] Loh NH, Tam SC, Miyazawa S. Statistical analyses of the effects of ball burnishing parameters on surface hardness. Wear 1989;129:235–43.
[3] Loh NH, Tam SC, Miyazawa S. Ball burnishing of tool steel. Precision Engineering 1993;15:100–5.
[4] Hassan AM, Maqableh AM. The effects of initial burnishing parameters on non-ferrous components. Journal of Materials Processing Technology 2000;102:115–21.
[5] Hassan AM, Al-Bsharat AS. Influence of burnishing process on surface roughness, hardness, and microstructure of some non-ferrous metals. Wear 1996;199:1–8.
[6] El-Axir MH. An investigation into roller burnishing. International Journal of Machine Tools and Manufacture 2000;40:1603–17.
[7] Luca L, Neagu-Ventzel S, Marinescu I. Effects of working parameters on surface finish in ball-burnishing of hardened steels. Precision Engineering 2005;29:253–6.
[8] El-Tayeb NSM, Low KO, Brevern PV. On the surface and tribological characteristics of burnished cylindrical Al-6061. Tribology International 2009;42:320–6.
[9] López de Lacalle LN, Lamikiz A, Sánchez JA, Arana JL. The effect of ball burnishing on heat-treated steel and Inconel 718 milled surfaces. The International Journal of Advanced Manufacturing Technology 2006;32:958–68.
[10] Luo H, Liu J, Wang L, Zhong Q. Study of the mechanism of the burnishing process with cylindrical polycrystalline diamond tools. Journal of Materials Processing Technology 2006;180:9–16.
[11] Röttger K. Walzen hartgedrehter oberflaechen. Aachen: RWTH; 2002.
[12] Yen YC, Sartkulvanich P, Altan T. Finite element modelling of roller burnishing process. CIRP Annals – Manufacturing Technology 2005;54:237–40.
[13] Zienkiewicz OC, Zhu JZ. A simple error estimator and adaptive procedure for practical engineering analysis. International Journal for Numerical Methods in Engineering 1987;24:337–57.
[14] Zienkiewicz OC, Taylor RL, Zhu JZ. Finite element method – its basis and fundamentals. 6th ed. Elsevier; 2005.
[15] Barquins M, Kennel M, Courtel R. Comportement de monocristaux de cuivre sous l'action de contact d'un frotteur hemisphèrique. Wear 1968;11: 87–110.